Front. Chem. China 2008, 3(2): 128–132
DOI 10.1007/s11458-008-0024-1

RESEARCH ARTICLE

Yingpin LI, Xiaoquan ZHOU, Huijing ZHOU, Zhurui SHEN, Tiehong CHEN

Hydrothermal preparation of nanostructured MnO_2 and morphological and crystalline evolution

Abstract Manganese dioxides with various morphologies were prepared using a common hydrothermal method without any templates or additives. The evolution of the morphology was accompanied by the gradual conversion of the polymorphic forms from γ-type to β-type. Meanwhile, MnO_2 microspheres, urchin-like nanostructures and nanowires were successfully synthesized. The products were characterized by X-ray diffraction, X-ray photoelectron spectroscopy, scanning electron microscope and transmission electron microscope. The evolution process can be explained by the Ostwald Ripening mechanism.

Keywords MnO_2, hydrothermal preparation, crystal type, core-shell structure, nanowires

1 Introduction

Nanostructured inorganic materials have special optical, electrical, mechanical and thermal properties, and have received more and more attention. MnO_2 as an important functional inorganic material has been widely used in the field of catalysts and electrode materials [1–4]. MnO_2 has many kinds of polymorphs, such as α-,β-,δ-,γ-, and ε-type when the basic unit [MnO_6] octahedron links in different ways. Up to now, 1D, 2D and 3D hierarchical MnO_2 have been reported. However, most of the work only studied a special MnO_2 morphology. Tang et al. [5] had obtained dandelion-like β-MnO_2. Xie et al. [6] and Li et al. [7] prepared sisal-like nanostructured γ-MnO_2 and urchin-like MnO_2 microspheres using a hydrothermal method. Zhou et al. [8] synthesized microsphere of aligned nanorods with PEG as directing agent.

The morphology of MnO_2 has an important effect on practical applications. Xie et al. [9] confirmed that α-MnO_2 hollow urchins performed better than other α-MnO_2 samples (solid urchins and dispersed nanorods) when using as a cathode material in Li-ion batteries. Yang et al. [10] reported that MnO_2 nanorods have good catalytic effect for methyl blue decomposition. Ma et al. [11] proved that the layered MnO_2 nanobelt is an ideal cathode material for rechargeable Li-ion batteries.

In this work, the simple hydrothermal method used for synthesizing MnO_2 nanowires and MnO_2 nanorods reported by Li et al. [12,13] was adopted. By changing the reaction time, the evolution process of the MnO_2 microstructure from sphere to sunflower, core-shell and finally to nanowire was studied and the evolution of the morphology and crystal transformation of the MnO_2 material was discussed.

2 Experimental

2.1 Reagents and instruments

$Mn(SO_4)_2$ (AR grade), was obtained from the Third Tianjin Chemical Regent Factory and $(NH_4)_2S_2O_8$ (AR grade) was from Tianjin Kermal Chemical Regent Co. Ltd. **A** Shimadzu SS-550 scanning electron microscope was used with a working voltage of 15 kV. A Rigaku D/max-2500 X-ray photoelectron spectroscope was used with a Cu Kα radial, a working voltage of 40 kV and a working current of 100 mA. **A** Kratos Axis Ultra DLD X-ray photoelectron instrument with X monochromic X-ray, a working voltage of 15 kV and a working current 10 mA was used. The pass energy of the wide spectra is 80 eV and the pass energy of the high resolution spectra is 40 eV. The binding energy of XPS spectra is calibrated by using contaminant carbon (C_{1S}, 284.6 eV).

2.2 Experimental process

Hydrated manganese sulfate ($MnSO_4 \cdot H_2O$, 0.008 mol) and an equal amount of ammonium persulfate ($(NH_4)_2S_2O_8$) were mixed with 20 ml distilled water at

Translated from *Chinese Journal of Chinese Universities* 28(7): 1223–1226 [译自: 高等学校化学学报]

Yingpin LI, Xiaoquan ZHOU, Huijing ZHOU, Zhurui SHEN, Tiehong CHEN (✉)
Department of Materials Chemistry, College of Chemistry, Nankai University, Tianjin 300071, China
E-mail: chenth@nankai.edu.cn

room temperature by magnetic stirring for 30 min. The mixture was transferred into a Teflon-lined stainless steel autoclave and maintained at 120°C at different reaction times (40 min–48 h). After cooling to room temperature, the mixture was filtrated and a black precipitate was obtained. The precipitate was washed with distilled water for several times and dried at 50°C for 36 h. Finally, a black powder product was obtained.

3 Results and discussion

3.1 X-ray power diffraction (XRD) characterization

Figure 1 shows the XRD patterns of the products obtained with different reaction times, and the diffraction peaks can be attributed to α-MnO_2, β-MnO_2 and γ-MnO_2. As shown in Fig. 1(a), the product obtained with a reaction time of 40 min was pure γ-MnO_2 (in accordance with JCPDS 14-0644). Judging from the weak and wide diffraction peaks, the γ-MnO_2 had a small size or low crystallinity. After a reaction time of 2 h, the main diffraction peaks of the product were attributed to γ-MnO_2 as shown in Fig. 1(b), and it also contained little α-MnO_2 (in accordance with JCPDS 44-0141) and β-MnO_2. After reaction time for 4 h, γ-MnO_2 decreased and β-MnO_2 increased in the product as shown in Fig. 1(c). After a reaction time of 24 h, the product was mainly β-MnO_2 and had little α-MnO_2 as shown in Fig. 1-(d). After a reaction time of 48 h, the product was pure β-MnO_2 as shown in Fig. 1(e) (in accordance with JCPDS 24-0725).

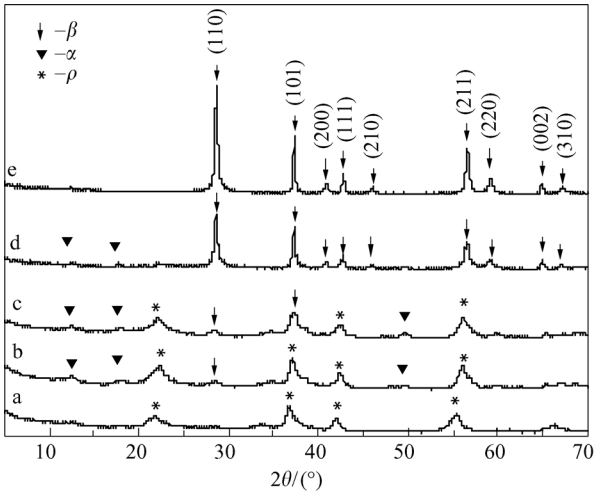

Fig. 1 XRD patterns of the products obtained with different reaction time. (a) 40 min; (b) 2 h; (c) 4 h; (d) 24 h; (e) 48 h

In this process, with the increase of the reaction time, the γ-MnO_2 gradually transformed to β-MnO_2**.** At the same time, α-MnO_2 appeared, and finally pure β-MnO_2 was obtained. When the reaction time was prolonged, the diffraction peaks gradually became narrow, indicating that the crystallinity was increased and the phase components become pure. Prolonging the reaction time was beneficial for the β-MnO_2 growth, indicating that β-MnO_2 was more stable than γ-MnO_2 in this system.

3.2 X-ray photoelectron spectroscopy (XPS) detection

The XPS spectroscopic results of MnO_2 after a reaction time of 48 h are shown in Fig. 2. It can be seen that the binding energy of $Mn_{2p1/2}$ and $Mn_{2p3/2}$ are 642.1 and 653.8, respectively, which are attributed to Mn^{4+}. The binding energy of O_{1s} is 529.5 eV, which is attributed to crystal lattice oxygen. This is consistent with the MnO_2 spectrum reported in the literature [14].

3.3 Scanning electron microscope (SEM) and transmission electron microscope (TEM) morphology observations.

From the scanning electron microscope observations, after a reaction time of 40 min, the diameter of the microsphere product was smaller than 5 um as shown in Fig. 3(a). Radially–aligned nanowires make up urchin-like spherical MnO_2 with diameters of about 4–8 um as shown in Figure 3(b); the yield was very high. When the reaction time was prolonged to 4 h, MnO_2 spheres made up of nanowire was also obtained as shown in Fig. 3(c). In the inset, the nanowire was longer than that obtained after a reaction time of 2 h. When the reaction time was prolonged to 24 h, the product had a complex morphology due to the further growth of the one-dimensional nanostructure as shown in Fig. 3(d), such as the core-shell type and the sunflower-like type made up of nanowires as shown in Fig. 3(e). When the reaction time was prolonged to 48 h, pure β-MnO_2 nanowire was obtained as shown in Fig. 3(f).

The product obtained after a hydrothermal reaction time of 48 h was observed by transmission electron microscopy (TEM) as shown in Fig. 4. The diameter of nanowire was about 10–20 nm and the length was about 500 nm.

3.4 Evolution process discussion

It can be deduced from the scanning electron microscopy (SEM) images and the XRD pattern that the formation of MnO_2 nanowire mainly goes through three processes as shown in Fig. 5: (1) solid spheres with a smooth surface change to an urchin-like sphere made up of nanowires. During this process the γ-MnO_2 within the microsphere is redissolved and recrystallized to form α-MnO_2 nanowires; (2) solid microspheres convert to urchin-like hollow microspheres, where γ-MnO_2 grow outward and form hollow microspheres; (3) The hollow

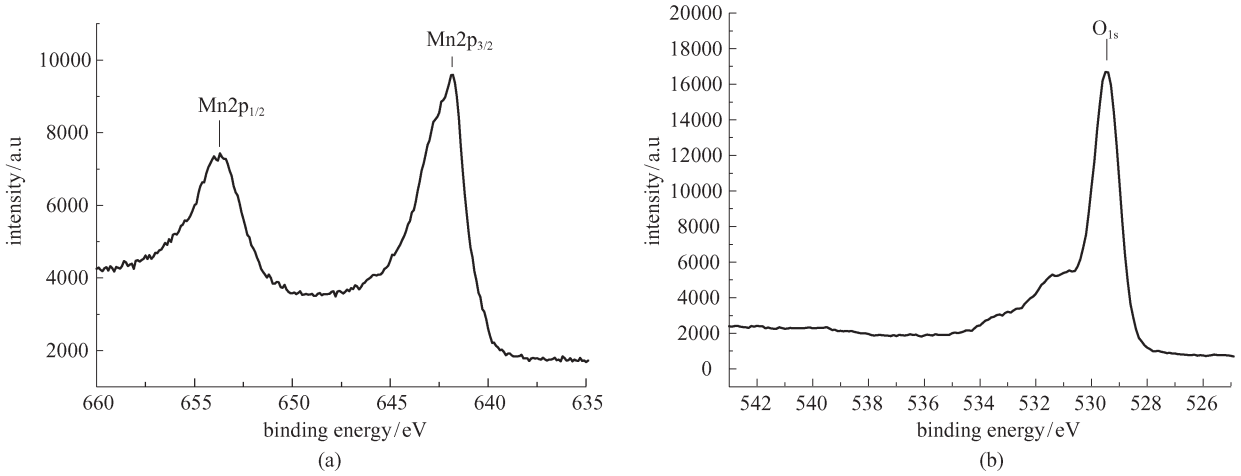

Fig. 2 XPS spectra of Mn_{2p} region and O_{1s} region of the product obtained with reaction time for 48 h

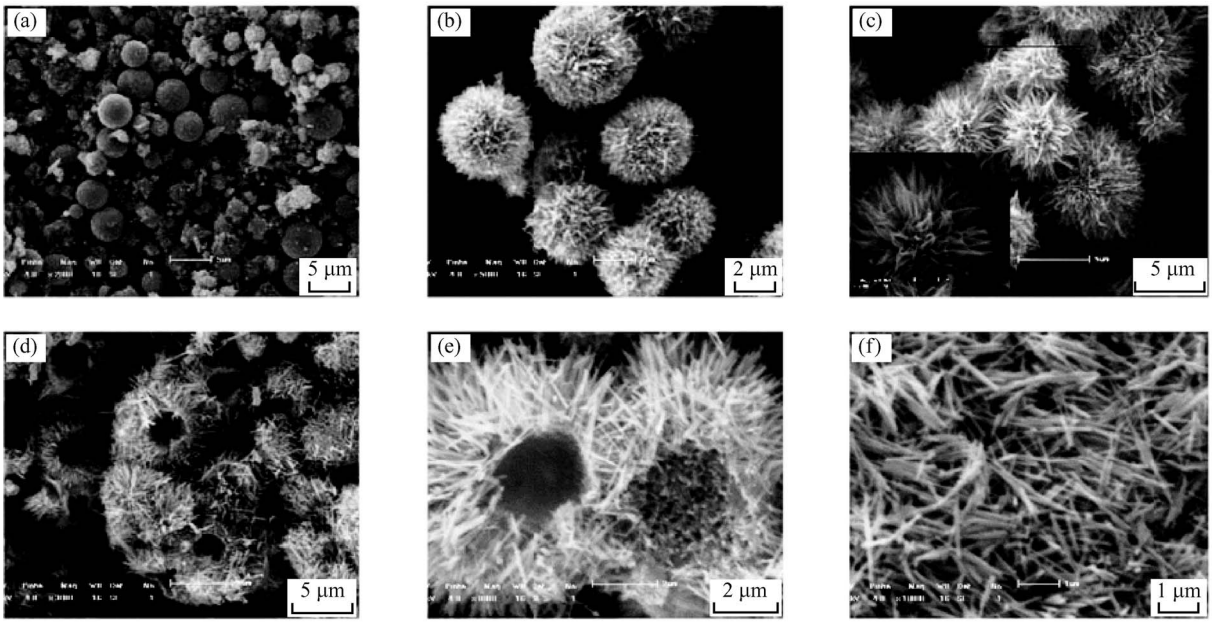

Fig. 3 SEM images of the products obtained with different reaction time
(a) 40 min; (b) 2 h; (c) 4 h; (d) 24 h; (e) 24 h; (f) 48 h

spheres which are made up of MnO_2 nanowire convert to nanowire. At this time, γ-MnO_2 continues growing outward, and finally the core-shell structure is destroyed and single β-MnO_2 nanowire are formed, as shown in Fig. 1(d). The XRD spectrum in Fig. 1 shows that the α-MnO_2 and γ-MnO_2 obtained gradually convert to β-MnO_2, and finally pure β-MnO_2 is obtained. At the same time, XPS analysis confirms that the product is pure MnO_2 as shown in Fig. 2. It can be concluded that the MnO_2 solid microspheres, under the Ostwald-Ripening effect [15] gradually convert to hollow spheres and finally to MnO_2 nanowires. Similar growth processes in the synthesis of ZnO and TiO_2 have been reported in literatures [16,17].

4 Conclusions

By changing the reaction time, different morphologies of MnO_2 was successively synthesized by using a hydrothermal method without any surfactant. The evolution of the crystal growth process was also studied. Because of the Ostward Ripening effect, MnO_2 crystals gradually form hollow core-shell spheres and finally form nanowires, accompanied by MnO_2 crystal type conversion. Because the microscopic morphology is important in the application of functional materials [18,19], MnO_2 materials with different morphologies prepared by this simple process have some potential application in the fields of electrochemistry and catalysts.

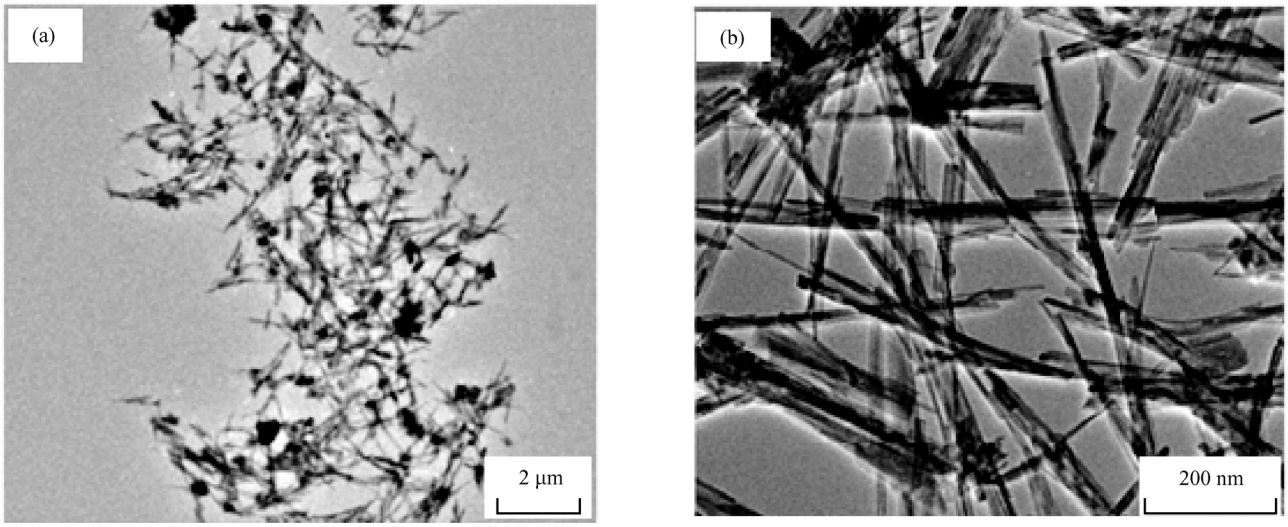

Fig. 4 TEM images of the nanowires obtained with reaction times of 48 h

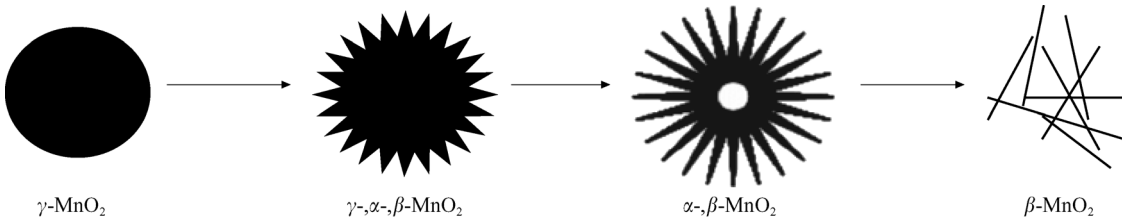

Fig. 5 Schematic illustration of the morphology evolution of MnO_2

References

1. A. Robert Armstrong, Peter G. Bruce. Synthesis of layered $LiMnO_2$ as an electrode for rechargeable lithium batteries. Nature, 1996, 381: 499–500
2. Zhan Hui, Zhou Yunhong. Studies on the properties of Li-Mn oxide made from various CMD. Chem J Chinese Universities, 2002, 23 (6): 1100–1104
3. Li Juan, Xia Xi, Li Qingwen. Synthesis and electrochemical properties of nanophase MnO_2 by solid-phase reaction (I) – synthesis and characterization of nanophase γ-MnO_2. Chem J Chinese Universities, 1999, 20(9): 1434–1437
4. Laura Espinal, Steven L Suib, James F. Rusling, Electrochemical catalysis of styrene epoxidation with films of MnO_2 nanoparticles and H_2O_2. J Am Chem Soc, 2004, 126(24): 7676–7682
5. Tang Bo, Wang Guangli, Zhuo Linhai, Ge Jiechao. Novel dandelion-like beta-manganese dioxide microstructures and their magnetic properties. Nanotechnology, 2006, 17: 947–951
6. Wu Changzheng, Xie Yi, Wang Dong, Yang Jun, Li Tanwei. Selected-control hydrothermal Synthesis of γ-MnO_2 3D nanostructures. J Phys Chem B, 2003, 107(49): 13583–13587
7. Li Zhengquan, Ding Yue, Xiong Yujie, Yang Qing, Xie Yi. One-step solution-based catalytic route to fabricate novel *a*-MnO_2 hierarchical structures on a large scale. Chem Commun, 2005: 918–920
8. Zhou Xingfu, Chen Shuyi, Zhang Danyu, Guo Xuefeng, Ding Weiping, Chen Yi. Microsphere organization of nanorods directed by PEG linear polymer. Langmuir, 2006, 22(4): 1383–1387
9. Li Benxia, Rong Guoxin, Xie Yi, Hung Lunfeng, Feng Chuanqi. Low-temperature synthesis of α-MnO_2 hollow urchins and their application in rechargeable Li^+ batteries. Inorg Chem, 2006, 45(16): 6404–6410
10. Yang Zeheng, Zhang Yuancheng, Zhang Weixin, Wang Xue, Qian Yitai, Wen Xiaogang, Yang Shihe. nanorods of manganese oxides: synthesis, characterization and catalytic application. Journal of Solid State Chemistry, 2006, 179: 679–684
11. By Renzhi Ma, Yoshio Bando, Zhang Lianqi, Takayoshi Sasaki. Layered MnO_2 nanobelts: hydrothermal synthesis and electrochemical measurements. Adv Mater, 2004, 16: 918–922
12. Wang Xun, Li Yadong. Selected-control hydrothermal synthesis of α- and β-MnO_2 single crystal nanowires. J Am Chem Soc, 2002, 124: 2880–2881
13. Wang Xun, Li Yadong. Synthesis and formation mechanism of manganese dioxide nanowires/nanorods. Chem Eur J, 2003, 9: 300–306
14. Wang Lianzhou, Nobuyuki Sakai, Yasuo Ebina, Kazunori Takada, and Takayoshi Sasaki. Inorganic multilayer films of manganese oxide nanosheets and aluminum polyoxocations: fabrication, structure, and electrochemical behavior. Chem Mate, 2005, 17: 1352–1357
15. Liu Bin, Zeng Huachun. Symmetric and Asymmetric Ostwald Ripening in the fabrication of homogeneous core–shell semiconductors. Small, 2005, 1: 566–571
16. Liu Bin, Zeng Huachun. Fabrication of ZnO "Dandelions" *via* a modified Kirkendall process. J Am Chem Soc, 2004, 126(51): 16744–16746
17. Yang Huagui, Zeng Huachun. Preparation of hollow anatase TiO_2 nanospheres via ostwald ripening. J Phys Chem B, 2004, 108: 3492–3495

18. Tang Yawen, Cao Shuang, Chen Yu, Bao Jianchun, Lu Tianhong. Effect of structure of carbon nanotubes on electrocatalytic performance of carbon nanotubes supported Pt catalysts. Chem J Chinese Universities, 2007, 28(5): 936–939

19. Liu Ping, Li Xinyong, Wang Yuxin, Ju Xiaodong, Chen Guohua. Construction and photoelectrocatalytic properties of TiO_2 nanotubes arrays on titanium substrates. J Chinese Universities, 2006, 27(12): 2411–2413